



■ BONE BIOLOGY

Cyclin D1 mediates pain behaviour in a rat model of breast cancer-induced bone pain by a mechanism involving regulation of the proliferation of spinal microglia

**X. Guan,
X. Gong,
Z. Y. Jiao,
H. Y. Cao,
S. Liu,
C. Lin,
X. Huang,
H. Lan,
L. Ma,
B. Xu**

*From The First Affiliated
Hospital of Guangxi
Medical University,
Nanning, China*

Aims

The involvement of cyclin D1 in the proliferation of microglia, and the generation and maintenance of bone cancer pain (BCP), have not yet been clarified. We investigated the expression of microglia and cyclin D1, and the influences of cyclin D1 on pain threshold.

Methods

Female Sprague Dawley (SD) rats were used to establish a rat model of BCP, and the messenger RNA (mRNA) and protein expression of ionized calcium binding adaptor molecule 1 (IBA1) and cyclin D1 were detected by reverse transcription-polymerase chain reaction (RT-PCR) and western blot, respectively. The proliferation of spinal microglia was detected by immunohistochemistry. The pain behaviour test was assessed by quantification of spontaneous flinches, limb use, and guarding during forced ambulation, mechanical paw withdrawal threshold, and thermal paw withdrawal latency.

Results

IBA1 and cyclin D1 in the ipsilateral spinal horn increased in a time-dependent fashion. Spinal microglia proliferated in BCP rats. The microglia inhibitor minocycline attenuated the pain behaviour in BCP rats. The cyclin-dependent kinase inhibitor flavopiridol inhibited the proliferation of spinal microglia, and was associated with an improvement in pain behaviour in BCP rats.

Conclusion

Our results revealed that the inhibition of spinal microglial proliferation was associated with a decrease in pain behaviour in a rat model of BCP. Cyclin D1 acts as a key regulator of the proliferation of spinal microglia in a rat model of BCP. Disruption of cyclin D1, the restriction-point control of cell cycle, inhibited the proliferation of microglia and attenuated the pain behaviours in BCP rats. Cyclin D1 and the proliferation of spinal microglia may be potential targets for the clinical treatment of BCP.

Cite this article: *Bone Joint Res* 2022;11(11):803–813.

Keywords: Cyclin D1, Bone cancer induced pain, Microglia, Proliferation, Spinal cord

Article focus

■ The purpose of this study was to examine whether cyclin D1 acts as a key regulator of the proliferation of spinal microglia in bone cancer pain (BCP) rats, and whether the disruption of cyclin D1 would inhibit the proliferation of microglia and attenuate the pain behaviours in BCP rats.

Key messages

- Inhibition of spinal microglial proliferation was associated with a decrease in pain behaviour in BCP rats.
- Cyclin D1 acts as a key regulator of the proliferation of spinal microglia in BCP rats.

Correspondence should be sent to
Xuehai Guan; email:
guan_xh@aliyun.com

doi: 10.1302/2046-3758.1111.BJR-
2022-0018.R1

Bone Joint Res 2022;11(11):803–
813.

- Disruption of cyclin D1 was associated with attenuation of pain behaviour in BCP rats.

Strengths and limitations

- This is the first study to confirm that cyclin D1 acts as a key regulator of the proliferation of spinal microglia in BCP rats, and disruption of cyclin D1 was associated with attenuation of pain behaviour in BCP rats.
- One limitation of our study was that we did not investigate the role of cyclin D1 and proliferation of microglia in BCP rats at supraspinal level.

Introduction

Bone cancer pain (BCP) is a common complication in patients with cancer bone metastasis or primary bone cancer.¹⁻⁶ BCP may be severe and difficult to adequately control by current drugs and therapeutic approaches, which illustrates that this clinical problem has not been solved.⁷ Thus, it is necessary to elucidate the molecular and cellular mechanisms of BCP.

A paradigm shift in understanding chronic pain has been the realization that neurones are not the only cells involved in the aetiology. Immune cells, such as glial cells, contribute to sensitization in pain pathway both in the central nervous system (CNS) and the peripheral nervous system (PNS). Microglia, the tissue-resident macrophages of the CNS, infiltrate and take up residence in the developing brain, actively engulf synaptic material, and play a major role in synaptic maturation during postnatal development.⁸ Recent research emphasizes the role of neuron-microglia interaction in neuropathic pain. The proliferation of spinal glia has been shown to regulate neuropathic pain.^{9,10} A correlation between pain behaviours and microglial activation has been reported,¹¹ although there are contradictory findings.¹² We have reported the correlation between BCP and microglia,¹³⁻¹⁵ but little is known about the mechanisms.^{7,13-16}

Disruption of restriction-point control may be a common biological feature in cancer treatment. Cyclins and their kinase partners regulate cell-cycle progression. For example, cyclin D1 regulated the proliferation of spinal astrocytes in a rat model of neuropathic pain.⁹ However, whether cyclin D1 participates in the generation and maintenance of BCP has not yet been clarified.

In the present study, we firstly established a rat model of BCP by injecting Walker 256 rat mammary gland carcinoma cells into the medullary canal of the tibia.^{13,15,17-19} Then we investigated the role of cyclin D1 in regulating the proliferation of spinal microglia and their role in pain behaviour in BCP rats. Our findings may elucidate the mechanisms of neuron-microglia interaction in BCP, and thereby provide novel targets for the clinical treatment of BCP.

Methods

Materials. A total of 300 female Sprague Dawley (SD) rats were purchased from the Experimental Animal Research Centre of Guangxi Medical University. Walker

256 rat mammary gland carcinoma cells (LLC-WRC 256) and polyethylene (PE)-10 catheters (PE-0503) were obtained from the Institute of Cancer Research of Chinese Academy of Medical Science and Peking Union Medical College, and Anilab (China), respectively. Minocycline (S4226) and flavopiridol (L86-8275) were obtained from Selleck chem (USA). D-Hank's solution (H1045) and Triton X-100 (T8200) were provided by Solarbio Life Sciences (China). RIPA (P0013B) and bicinchoninic acid (BCA) assay (P0012) were supplied by Beyond (China). Polyvinylidene fluoride membrane was purchased from Merck Millipore (Germany). Horseradish peroxidase (HRP)-conjugated donkey anti goat immunoglobulin G (IgG) (bs-0294D) was obtained from Bioss (China). Rabbit anti-glyceraldehyde 3-phosphate dehydrogenase (GAPDH) (ab181602), rabbit anti-Ki67 (ab15580), rabbit anti-cyclin D1 (ab156448), rabbit anti p-HisH3 (ab5176), polyclonal anti-IBA1 (ab5076), CY3-conjugated donkey anti-goat IgG (ab6949), Alexa Fluor 488-conjugated donkey anti-rabbit IgG (ab150073), and HRP-conjugated goat anti-rabbit IgG (ab136817) were acquired from Abcam (UK). TRizol reagent (#15596026) and 4',6-diamidino-2-phenylindole (DAPI, Cat# D1306) were provided by Thermo Fisher Scientific (USA). The specific primer sequences of IBA1 and GAPDH were designed and synthesized by Takara (Japan).

Ethical statement and experimental design. All experimental protocols were approved by the Animal Care and Use Committee of our hospital and were in accordance with the Declaration of the National Institutes of Health Guide for Care. We have included an ARRIVE checklist to show that we have conformed to the ARRIVE guidelines. Adult female SD rats (weighing 180 to 220 g; Supplementary Figure a) were housed under a 12 hr/12 hr light-dark cycle regime at a constant temperature of 22°C ± 1°C with ad libitum access to food and water. Animals were randomly allocated to the following groups: 1) Sham, 2) BCP, 3) BCP-Vehicle, 4) BCP-MC, and 5) BCP-Flavo. Ten rats were assigned to each group for behavioural testing, and four rats were assigned to each group at various timepoints for different molecular experiments.

Preparation of carcinoma cells and BCP model. The preparation of Walker 256 rat mammary gland carcinoma cells and the BCP procedure were carried out as previously described.^{13,15,19} Briefly, carcinoma cells were inoculated into the abdominal cavity of female rats and extracted from the ascites after seven days, rinsed in D-Hank's solution, and centrifuged at 500 g for five minutes at 4°C (four cycles). Then, the pellet was calibrated at a concentration of 4 × 10⁵ cells/ml and maintained on ice until inoculation. Under anaesthesia with pentobarbital sodium (50 mg/kg, intraperitoneal), rats were laid in the supine position. The right leg was shaved and disinfected with 7% iodine. The plateau of the tibia was exposed with a small incision. A 23-gauge needle was inserted into the medullary canal of the tibia. Then, the needle was replaced with a thin blunt needle attached to a 10 µl Hamilton syringe. A 10 µl volume containing approximately 4 × 10⁴ live cells (BCP

model) or heat-killed cells (denatured at 95°C for five minutes, Sham model) was slowly injected into the bone cavity. The injected site was sealed with bone wax after the syringe was retracted. The skin was sutured with 3/0 silk thread and dusted with penicillin antibiotic powder. All rats were placed on a heated pad until recovery from anaesthesia, and then transferred into their cages.

Intrathecal catheterization and drug administration. Intrathecal catheterization was performed as described previously.^{15,20} Under pentobarbital sodium (50 mg/kg, i.p.) anaesthesia, a PE-10 catheter (outer diameter 0.6 mm, inner diameter 0.3 mm) was implanted through a gap in the vertebrae between L5 and L6, extending to the subarachnoid space. The catheter position was determined by intrathecal injection of 1% lidocaine (5 µl). If there is no hind limb paralysis within five minutes after intrathecal injection of lidocaine, the animal is considered as failure of catheterization. Animals with neurological deficits (eight rats) or failed catheterization (eight rats) were excluded from further experimentation. Minocycline (4, 20, or 100 µg/10 µl, once a day, from postoperative day 3 to 15), flavopiridol (0.04, 0.2, or 1 µg/10 µl, once a day, from postoperative day 3 to 15), or vehicle (10 µl) was intrathecally injected (i.t.) via the implanted catheter in a 10 µl volume followed by 10 µl sterile saline for flushing, lasting at least three minutes. The dosage was based on our preliminary experiments.

Behavioural testing. All behavioural tests and data analysis were performed under double-blind condition by two experimenters (ZYJ and HYC) who did not know the group allocation and the treatments. Rats were acclimated for 30 minutes in a quiet room before behavioural tests. The behavioural tests were performed before drug administration at days 0 (before the operation), 5, 10, 15, and 20 after carcinoma cell injection. Quantification of spontaneous flinches over a two-minute period was used to measure ongoing pain.^{14,21} Limb use during normal ambulation in an open field and guarding during forced ambulation were used to evaluate movement-evoked pain.^{14,21} Briefly, forced ambulatory guarding was measured using a rotarod and was scored on a scale of 5 to 0.^{14,21} 5, complete lack of use of limb; 4, partial non-use of limb; 3, substantial limping and prolonged guarding of limb; 2, substantial limping; 1, some limping, but not substantial; and 0, normal use of limb. Limb use was rated on a scale of 4 to 0: 4, normal use; 3, substantial limping; 2, limping and guarding behaviour; 1, partial non-use of the limb in locomotor activity; and 0, complete lack of limb use.

Mechanical paw withdrawal threshold (PWT) was measured by using von Frey filaments (1, 1.4, 2, 4, 6, 8, 10, and 15 g bending force; Stoelting, USA), starting with 1 g and ending with 15 g in ascending order.^{14,22} Each monofilament was applied five times, for a duration of one second and at ten-second intervals. Paw-flinching or quick withdrawal was considered as a positive response. The paw withdrawal frequency (PWF) to each monofilament was calculated from five applications. PWT was

determined by the force at which PWF \geq 60%; 15 g was recorded as the PWT if PWF < 60% to all filaments.

Paw withdrawal latency (PWL) from a radiant heat machine was used to measure the thermal hyperalgesia according to the method described by Hargreaves et al.^{14,23-25} In brief, rats were acclimated to the test chamber for one hour on a glass platform at 25°C. Radiant heat was focused on the area of the ipsilateral paw from underneath the glass. The time required to cause an abrupt withdrawal of the ipsilateral paw was regarded as the PWL.

Western blot. Rats were deeply anaesthetized by intraperitoneal injection of sodium pentobarbital (60 mg/kg). The ipsilateral and contralateral spinal cord at L3-5 segments was homogenized in radio immunoprecipitation assay (RIPA) lysis buffer (250 µl). The homogenized samples were centrifuged at 12,000 g for 30 minutes at 4°C. The concentration of the supernatant was determined by BCA assay. Samples were dissolved in 5× sample buffer (125 mM Tris, 10% sodium dodecyl sulphate (SDS), 0.25% bromophenol blue, 10% 2-Mercaptoethanol, 50% Glycerol) and denatured at 95°C for five minutes. Samples containing 30 µg protein were separated by SDS-PAGE gel (10% to 15%) and transferred onto polyvinylidene fluoride membranes. Membranes were blocked in 5% bovine serum albumin (BSA) in tris-buffered saline with Tween-20 (TBST) for two hours at room temperature, incubated overnight at 4°C with the following primary antibodies: goat anti-IBA1 (1:1,000), rabbit anti cyclin D1 (1:1,000), rabbit anti-GAPDH (1:5,000) made in the blocking solution, and then further incubated with HRP-conjugated secondary antibodies for two hours at room temperature. Target protein bands were visualized using chemiluminescence and measured by an Odyssey Fc Image System (LI-COR Biosciences; Imaging software: Image Studio Ver 5.2, USA).

Real-time quantitative PCR. Total RNA was extracted from ipsilateral and contralateral spinal cords (L3-5) using TRIzol reagent. The synthesis and real-time PCR were performed as previously described.¹⁹ GAPDH was used as an internal control. The expression level of target mRNA was quantified relative to GAPDH by using the comparative quantification 2^{-ΔΔCT} method. The specific primer sequences were designed and synthesized by Takara: IBA1-TGGCTCCGAGGAGACGTTTCAG (forward), ACTCTGGC TCACAACTGCTTCTTC (reverse); GAPDH-GGCACAGT CAAGGCTGAGAATG (forward), and ATGGTGGTGAAG ACGCCACTA (reverse).

Immunohistochemistry. Rats were deeply anaesthetized by intraperitoneal injection of sodium pentobarbital (60 mg/kg), and perfused transcardially with 200 ml saline, followed by 200 ml of ice-cold paraformaldehyde (4%) in phosphate-buffered saline (PBS). The L3-5 segments of the spinal cord were dissected and post-fixed in 4% paraformaldehyde for 24 hours, and subsequently allowed to equilibrate in 30% sucrose in PBS overnight at 4°C. A total of 20 µm transverse sections were cut on a cryostat (Leica, Germany) and every fifth section was

mounted on gelatine-coated slides. After washing with PBS, the sections were penetrated with 0.3% Triton X-100 at room temperature (RT) for 15 minutes. Non-specific binding was blocked by incubation in 5% normal donkey serum in PBS at RT for 60 minutes. Sections were incubated in the following primary antibodies: rabbit anti-Ki67 (1:200), rabbit anti-cyclin D1 (1:300), rabbit anti-p-HisH3 (1:200), and polyclonal goat anti-IBA1 (IBA1; microglia marker, 1:300). All sections were incubated at 4°C overnight. After washing with PBS (3 × 5 minutes), the sections were incubated with a mixture of CY3-conjugated donkey anti-goat IgG (1:300) and Alexa Fluor 488-conjugated donkey anti-rabbit IgG (1:300) secondary antibodies at 37°C for two hours. For nuclear staining, 4'-6-diamidino-2-phenylindole (DAPI; 500 ng/ml) was used in the last ten minutes before a final PBS wash (3 × 5 minutes). Non-specific labelling was determined running the same protocol without incubating with the primary antibodies. Sections were then mounted and cover-slipped with 75% glycerol in the dark. Images were taken using a fluorescence microscope (BX51, Olympus; Imaging software: cell Sens Standard 1.5, Japan).

To analyze alterations of positive cells, every fifth section was selected from a series of consecutive sections for each rat, and the total number of positive cells in the ipsilateral lamina (I-IV) were counted. The mean number (standard error of the mean (SEM)) in each section represented the change of positive cells.

Statistical analysis. The number of rats used in each experiment was based on the experience of Guan et al¹⁴ and Xu et al^{24–28} with this design. No a priori statistical power calculation was used to estimate the sample size. Differences were analyzed by GraphPad Prism 5.01 software (USA). Two-way analysis of variance (ANOVA) or one-way ANOVA with Bonferroni post hoc tests were used where appropriate. ‘Time’ was treated as ‘within subjects’ factor, and ‘Drug’ was treated as a ‘between’ subject factor. *F* values are expressed with degrees of freedom (DF) of treatment, time, interaction/residual. The criterion for statistical significance was $p < 0.05$.

Results

Spinal microglia were activated in BCP rats. To determine whether microglia were activated in BCP rats, we assessed mRNA and protein of IBA1 (biomarker of microglia) in the ipsilateral side of the spinal cord dorsal horn by real-time PCR, western blot, and immunofluorescence. Compared with the sham controls, the mRNA and protein of IBA1 increased starting at five days after carcinoma cell injection (Figures 1a to 1c). Expression of IBA1 on the contralateral side of the dorsal horn did not change significantly between BCP and sham controls (data are not shown).

Minocycline attenuated the pain behaviour in BCP rats. Although microglia were activated, their role in BCP is still unclear. Minocycline, one member of the tetracycline class of antibiotics, has been found to be a potent analgesic by selectively inhibiting microglia, besides its antimicrobial activity. In order to define the involvement

of spinal microglia in BCP, we examined the capacity of intrathecal delivery of minocycline to attenuate pain behaviour in BCP rats. Minocycline (4, 20, and 100 µg in 10 µl of 5% dimethyl sulfoxide (DMSO)) was administered intrathecally from days 3 to 15 after carcinoma cell injection. The treatment of minocycline showed a dose-dependent recovery in the decreased paw withdrawal threshold (Figure 1d), paw withdrawal latency (Figure 1e), limb use scores (Figure 1h), or in the increased number of spontaneous flinches (Figure 1f) and activity-related guarding scores (Figure 1g). After the last administration of minocycline on day 15, the significant attenuation of pain behaviours remained on day 20 (analyzed using two-way ANOVA: paw withdrawal threshold (Figure 1d, $p < 0.001$), paw withdrawal latency (Figure 1e, $p < 0.001$), number of spontaneous flinches (Figure 1f, $p < 0.001$), activity-related guarding scores (Figure 1g, $p < 0.01$), and limb use scores (Figure 1h, $p < 0.01$)).

Microglia proliferated in BCP rats. To visualize the proliferating cells in the lumbar dorsal horn, we performed immunohistochemical experiments by using Ki67-biomarker protein expressed in all phases of the cell cycle, excluding the resting phase. The number of Ki67+/DAPI+ cells in the ipsilateral dorsal horn increased significantly in a time-dependent manner, starting at day 10 after carcinoma cell injection ($p < 0.001$; Figures 2a to 2f), whereas the numbers in the contralateral side and sham rats were just slightly increased (data not shown). To identify the cell type of Ki67+/DAPI+ cells, we performed triple immunolabelling for cell type-specific markers. Most Ki67+/DAPI+ cells were labelled with IBA1 (a microglia marker, Figures 2a to 2f), but not with NeuN (a neuronal marker, data not shown) or glial fibrillary acidic protein (GFAP) (an astrocyte marker, data not shown).

To determine the mitotic phase of cycling microglia, we performed immunohistochemical experiments by using p-HisH3, a biomarker for the G₂/M phase of the cell cycle. As shown in Figures 2g to 2l, the number of p-HisH3+/DAPI+ cells in the ipsilateral dorsal horn increased significantly in a time-dependent manner, starting at day 5 after BCP, peaking at day 20 ($p < 0.001$, one-way ANOVA), whereas the numbers in the contralateral side and sham rats were just slightly increased (data not shown). Most p-HisH3+/DAPI+ cells were colocalized with microglia (Figures 2g to 2l), but not with neurones or astrocytes (data not shown).

Cyclin D1 is the biomarker protein expressed in the G1 or G₂/M transition. Compared with the sham controls, the mRNA (Figure 3a) and protein (Figures 3b and 3c) of cyclin D1 increase started at five days after carcinoma cell injection. Expression of cyclin D1 in the contralateral side of the dorsal horn did not change significantly between BCP and sham controls (data not shown). The number of IBA+/DAPI+ cells and cyclin D1+/DAPI+ cells in the ipsilateral dorsal horn increased significantly in a time-dependent manner, starting at day 10 after BCP, peaking at day 20 ($p < 0.001$, one-way

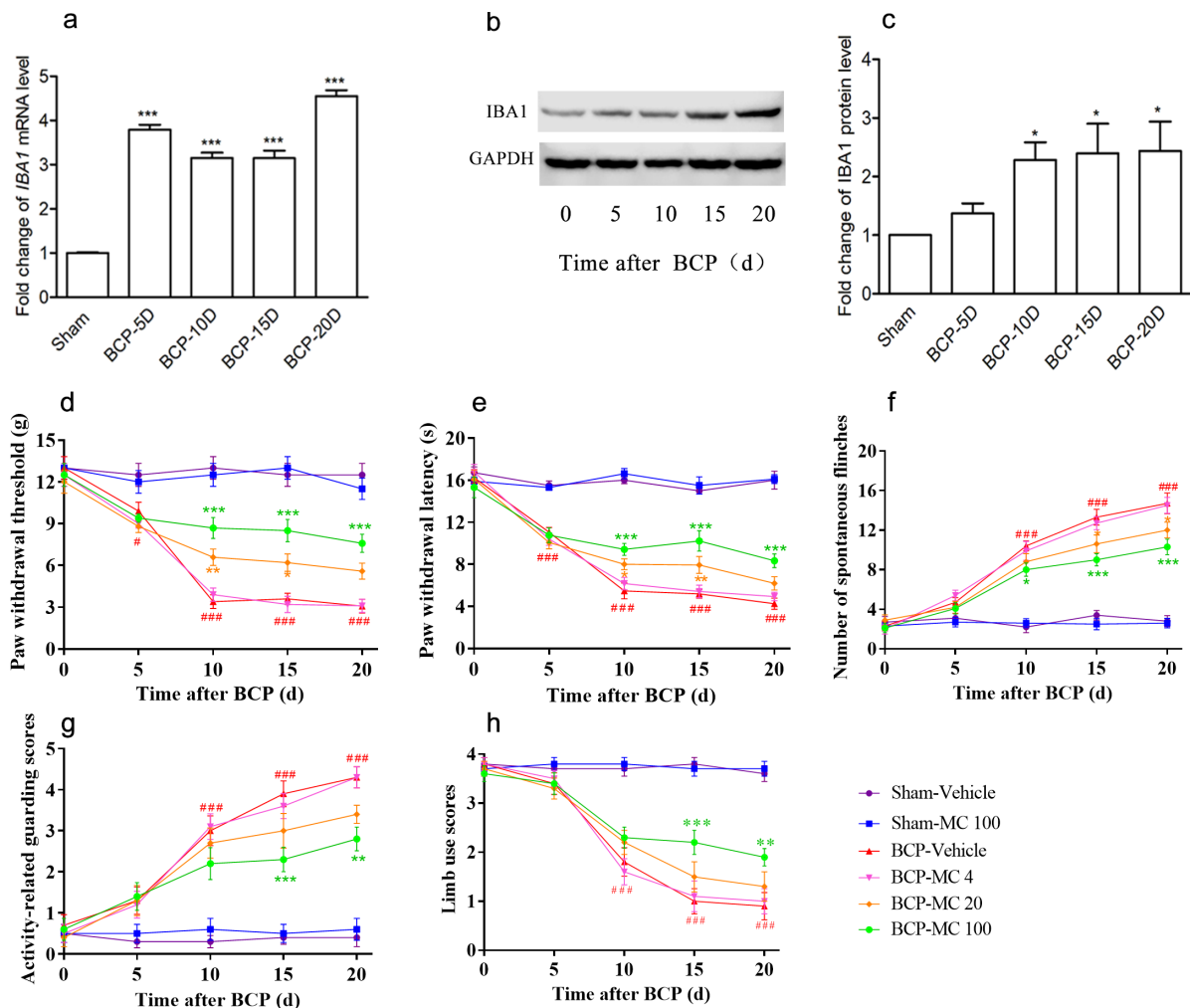


Fig. 1

The activation of spinal microglia and the effects of microglia inhibitor on pain behaviours in bone cancer pain (BCP) rats. a) The messenger RNA (mRNA) expression of ionized calcium binding adaptor molecule 1 (IBA1) was analyzed by real-time polymerase chain reaction (PCR). b) The representative bands and c) the quantitative data for the protein expression of IBA1 in the ipsilateral spinal cord at different timepoints after carcinoma cell injection were detected by western blot. The fold change of IBA1 was normalized to glyceraldehyde 3-phosphate dehydrogenase (GAPDH) of each sample. The fold change of IBA1 in the sham group was set at 1 for quantification. a) to c) * $p < 0.05$, *** $p < 0.001$ versus Sham group, analyzed using one-way analysis of variance (ANOVA) ($n = 4$). Minocycline (MC) (4, 20, or 100 $\mu\text{g}/10 \mu\text{l}$ intrathecally, once a day) or vehicle (10 μl) was administered for 13 days (from postoperative day 3 to 15). The behaviour tests were performed before drug administration at days 0 (before the operation), 5, 10, 15, and 20 after carcinoma cell injection. d) Paw withdrawal threshold (measured mechanical allodynia), e) paw withdrawal latency (measured thermal hyperalgesia), f) number of spontaneous flinches (measured ongoing pain). g) Decreases in activity-related guarding scores, and h) limb use scores during normal ambulation (evaluated movement-evoked pain) were prevented by minocycline in a dose-dependent manner- * $p < 0.05$, ** $p < 0.01$, *** $p < 0.001$ versus BCP-vehicle group; # $p < 0.05$, ### $p < 0.001$ versus Sham-vehicle group analyzed using two-way ANOVA ($n = 10$). d) Drug: $F(4, 216) = 64.81$, $p < 0.0001$; Time: $F(5, 54) = 74.78$, $p < 0.0001$; Drug \times Time: $F(20, 216) = 8.148$, $p < 0.0001$; e) Drug: $F(4, 216) = 125.0$, $p < 0.0001$; Time: $F(5, 54) = 132.5$, $p < 0.0001$; Drug \times Time: $F(20, 216) = 14.28$, $p < 0.0001$; f) Drug: $F(4, 216) = 131.9$, $p < 0.0001$; Time: $F(5, 54) = 93.04$, $p < 0.0001$; Drug \times Time: $F(20, 216) = 14.22$, $p < 0.0001$; g) Drug: $F(4, 216) = 55.71$, $p < 0.0001$; Time: $F(5, 54) = 76.07$, $p < 0.0001$; Drug \times Time: $F(20, 216) = 6.547$, $p < 0.0001$; and h) Drug: $F(4, 216) = 85.79$, $p < 0.0001$; Time: $F(5, 54) = 45.28$, $p < 0.0001$; Drug \times Time: $F(20, 216) = 9.393$, $p < 0.0001$. NS, normal saline.

ANOVA; Figures 3d to 3i), whereas the numbers in the contralateral side and sham rats were just slightly increased (data not shown). Most cyclin D1⁺/DAPI⁺ cells were colocalized with microglia (Figure 3i), but not with neurones or astrocytes (data not shown).

Effects of the cyclin-dependent kinase inhibitor flavopiridol on microglia proliferation and pain behaviours in BCP rats. If the proliferation of spinal microglia contributed to pain behaviour in BCP rats, interfering with

microglia cycling should alleviate the pain behaviours. To test this hypothesis, we conducted a test by using flavopiridol, a cell cycle inhibitor that inhibited glia proliferation in vivo and in vitro.⁹ Flavopiridol reduces cyclin D1 mRNA transcription, and arrests cells in G1 or G2/M transition.²⁹ Flavopiridol (1 μg , in 10 μl of 5% DMSO, once a day, i.t.) was administered intrathecally from days 3 to 15 after carcinoma cell injection. On day 15 after the last administration of flavopiridol, a series

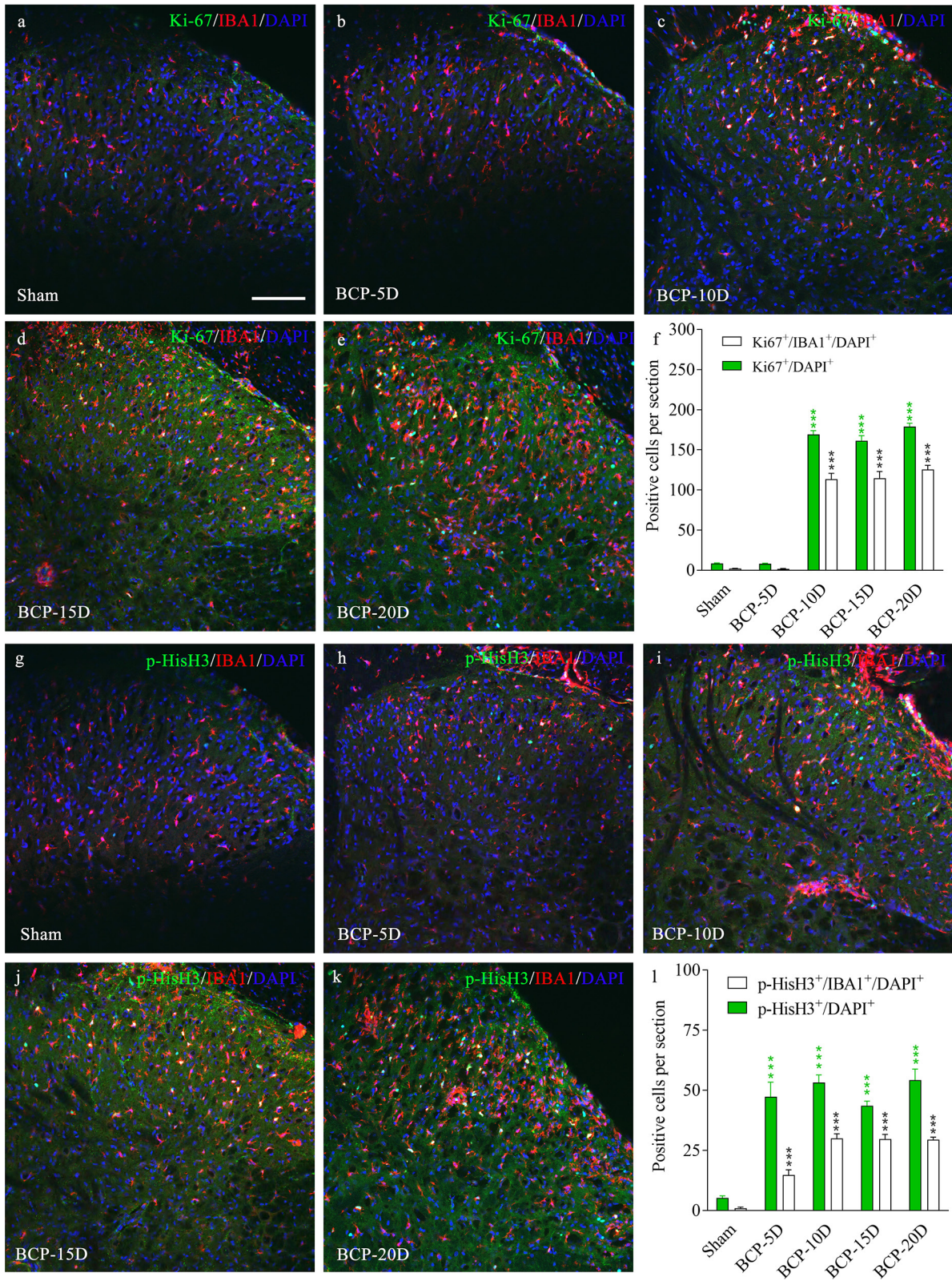


Fig. 2

Triple immunohistochemical characterization of proliferating microglia in the ipsilateral dorsal horn in bone cancer pain (BCP) rats. Ki67 is a nuclear protein expressed in all cell cycle phases except the resting phase. P-HisH3 is a marker protein expressed in the G2/M phase of the cell cycle. a) to f) The number of Ki67⁺/4'6-diamidino-2-phenylindole (DAPI⁺) cells, Ki67⁺/ionized calcium binding adaptor molecule 1 (IBA1⁺)/DAPI⁺ cells, and g) to l) p-HisH3⁺/DAPI⁺ cells and p-HisH3⁺/IBA1⁺/DAPI⁺ cells increased in the ipsilateral dorsal horn sections on days 10, 15, and 20 after carcinoma cell injection. ****p* < 0.001 versus the Sham group (analyzed using one-way analysis of variance (ANOVA); *n* = 4). Scale bar = 100 μ m.

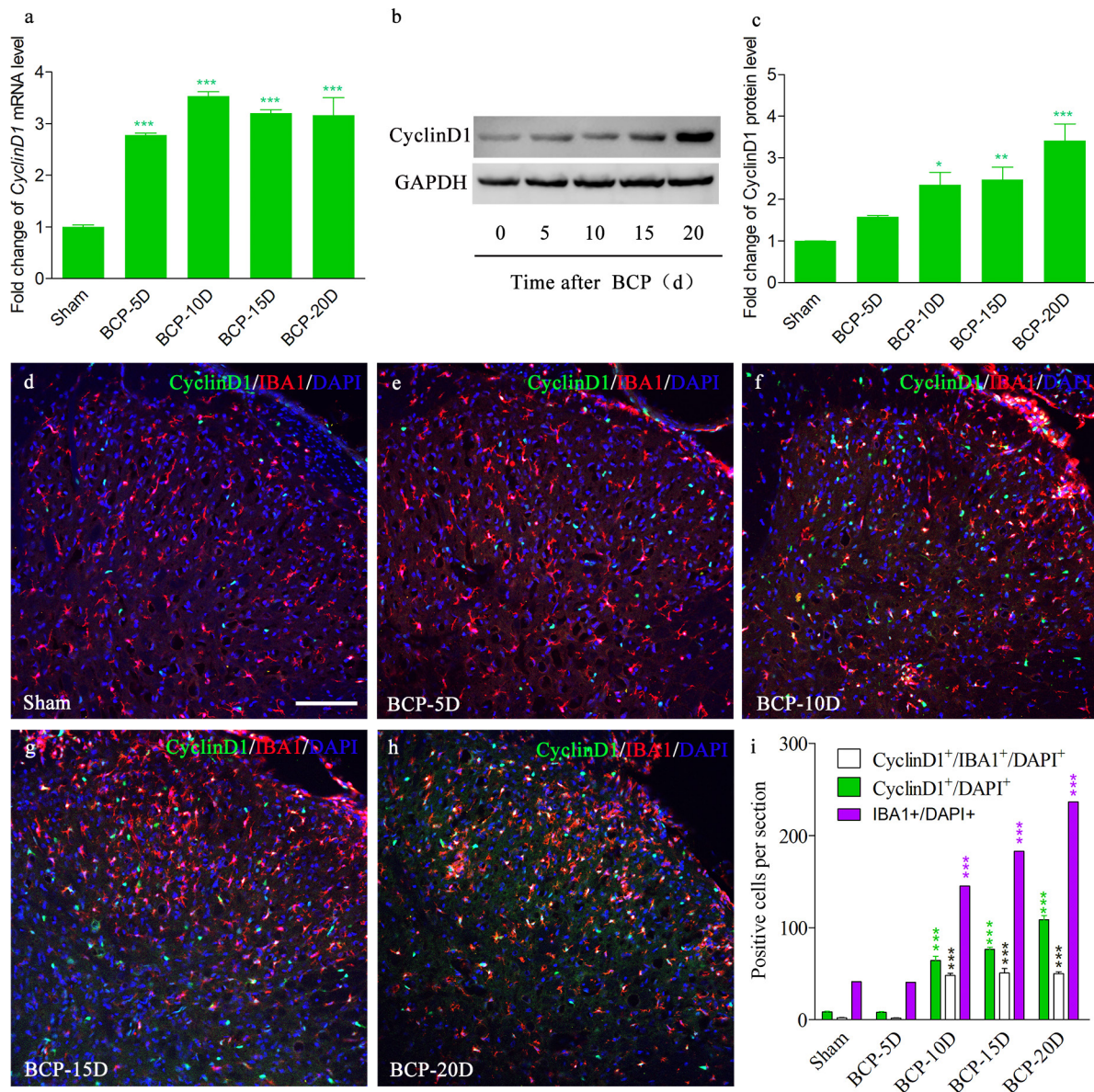


Fig. 3

The expression of spinal cyclin D1 in bone cancer pain (BCP) rats. a) The messenger RNA (mRNA) expression of ionized calcium binding adaptor molecule 1 (*IBA1*) was analyzed by real-time polymerase chain reaction (PCR). b) The representative bands and c) the quantitative data for the protein expression of cyclin D1 in the ipsilateral spinal cord at different timepoints after carcinoma cell injection were detected by western blot. The fold change of cyclin D1 was normalized to glyceraldehyde 3-phosphate dehydrogenase (GAPDH) of each sample. The fold change of cyclin D1 in the sham group was set at 1 for quantification. Cyclin D1 is colocalized with proliferating microglia in the dorsal horn in BCP rats. d) to i) The number of IBA1⁺/4'-6-diamidino-2-phenylindole (DAPI)⁺ cells, cyclin D1⁺/DAPI⁺ cells, and cyclin D1⁺/IBA1⁺/DAPI⁺ cells increased in the ipsilateral dorsal horn sections on days 10, 15, and 20 after carcinoma cell injection. **p* < 0.050, ***p* < 0.010, ****p* < 0.001 versus the Sham group (analyzed using one-way analysis of variance (ANOVA); *n* = 4). Scale bar = 100 μm.

of molecular tests were conducted. Compared with BCP-vehicle, flavopiridol attenuated the increase of the mRNA (Figure 4a) and protein (Figures 4b and 4c) of cyclin D1, decreased the number of IBA1⁺/DAPI⁺ cells, cyclin D1⁺/DAPI⁺ cells, and cyclin D1⁺/IBA1⁺/DAPI⁺ cells in the ipsilateral dorsal horn significantly (Figures 4d to 4f). Also, the number of Ki67⁺/DAPI⁺ cells, Ki67⁺/IBA1⁺/DAPI⁺ cells, p-HisH3⁺/DAPI⁺ cells, and p-HisH3⁺/IBA1⁺/DAPI⁺ cells in the ipsilateral dorsal horn on day 15 were

significantly lower in BCP-flavopiridol rats than in BCP-vehicle rats (*p* < 0.01, one-way ANOVA; Figures 4g to 4l).

Behaviourally, rats with BCP treated with flavopiridol from days 3 to 15 showed a significant recovery in the decreased paw withdrawal threshold (Figure 5a), paw withdrawal latency (Figure 5b), limb use scores (Figure 5e), or in the increased number of spontaneous flinches (Figure 5c) and activity-related guarding

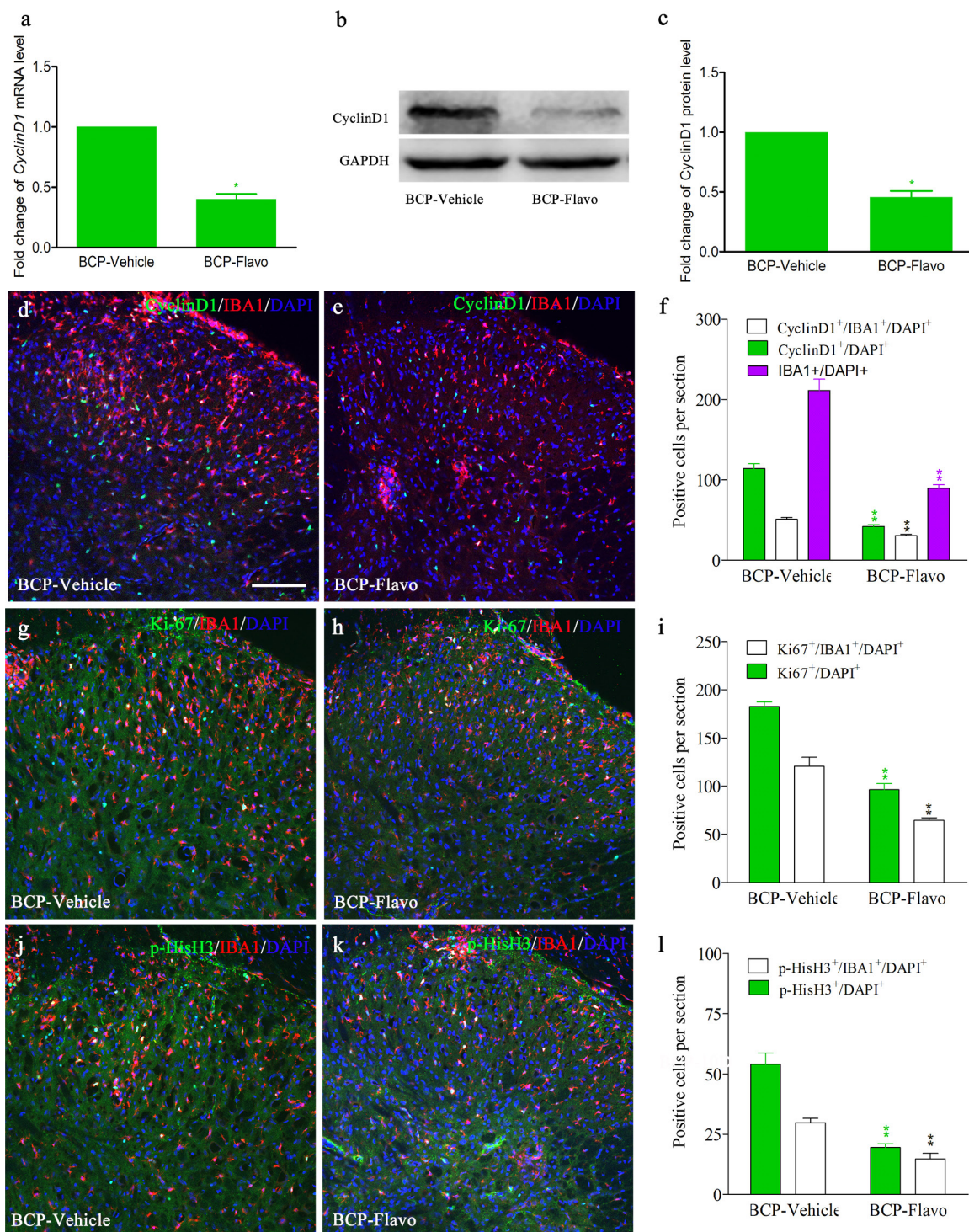


Fig. 4

Effects of the cell cycle inhibitor flavopiridol (Flavo) on microglia proliferation in bone cancer pain (BCP) rats. The cell cycle inhibitor, flavopiridol (i.t. 1 µg/10 µl, once a day) or vehicle (10 µl) was administered for 13 days (from postoperative day 3 to 15). After the last injection at day 15, ipsilateral L3-5 spinal cord was obtained to detect the effect of flavopiridol on microglia proliferation. Flavopiridol decreased the a) messenger RNA (mRNA) and b) and c) protein expression of cyclin D1. The fold change of cyclin D1 was normalized to glyceraldehyde 3-phosphate dehydrogenase (GAPDH) of each sample. The fold change of cyclin D1 in the BCP-vehicle group was set at 1 for quantification. d) to l) Flavopiridol decreased the number of ionized calcium binding adaptor molecule 1 (IBA1⁺)/4'6-diamidino-2-phenylindole (DAPI⁺) cells, cyclin D1⁺/IBA1⁺/DAPI⁺ cells, cyclin D1⁺/DAPI⁺ cells, Ki67⁺/DAPI⁺ cells, Ki67⁺/IBA1⁺/DAPI⁺ cells, p-HisH3⁺/DAPI⁺ cells, and p-HisH3⁺/IBA1⁺/DAPI⁺ cells in the dorsal horn on day 15. **p* < 0.05 ***p* < 0.01 versus the BCP-vehicle group (*n* = 4). Scale bar = 100 µm.

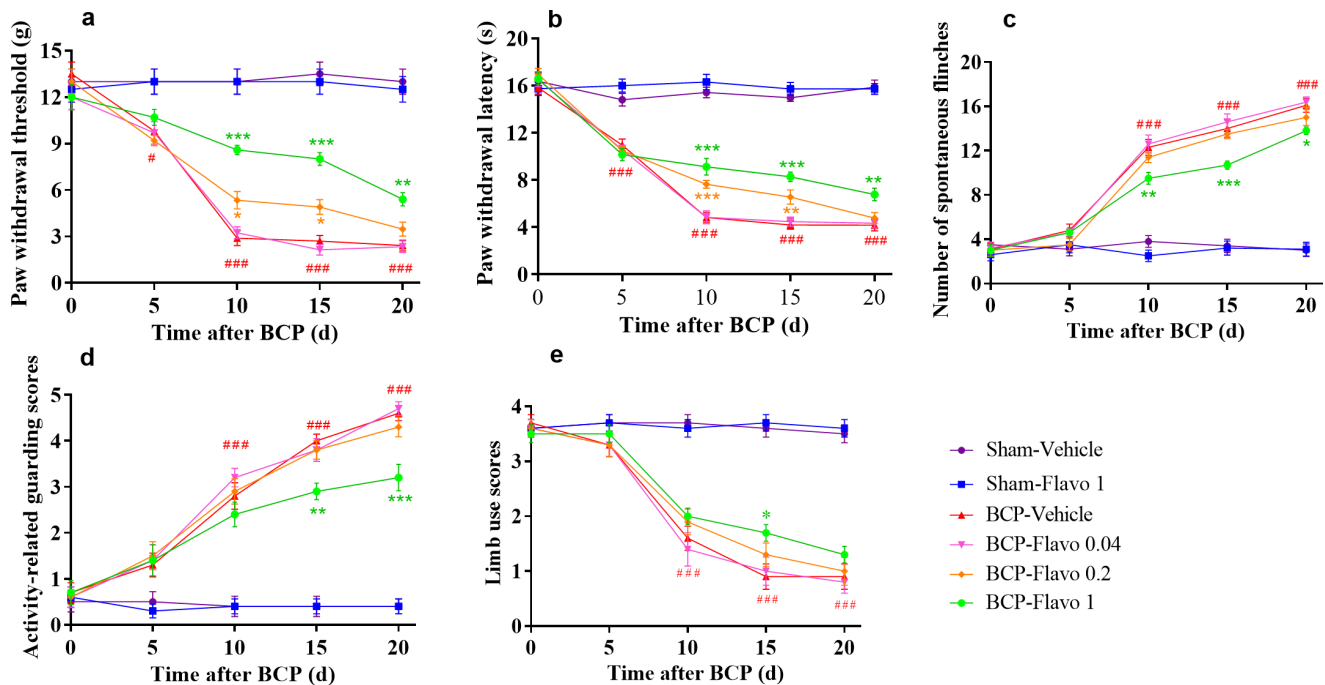


Fig. 5

Effects of the cell cycle inhibitor flavopiridol (Flavo) on pain behaviours in bone cancer pain (BCP) rats. The cell cycle inhibitor, flavopiridol (i.t. 0.04, 0.2, or 1 $\mu\text{g}/10\ \mu\text{l}$, once a day) or vehicle (10 μl) was administered for 13 days (from postoperative day 3 to 15). The behaviour tests were performed before drug administration at days 0 (before operation), 5, 10, 15, and 20 after carcinoma cell injection. a) Paw withdrawal threshold (measured mechanical allodynia), b) paw withdrawal latency (measured thermal hyperalgesia), c) number of spontaneous flinches (measured ongoing pain), d) activity-related guarding scores, and e) limb use scores during normal ambulation (evaluated movement-evoked pain) were prevented by flavopiridol. Analyzed using two-way analysis of variance (ANOVA), * $p < 0.05$, ** $p < 0.01$, *** $p < 0.001$ versus BCP-vehicle group; # $p < 0.05$, ### $p < 0.001$ versus Sham-vehicle group ($n = 10$). a) Drug: $F(4, 216) = 97.90$, $p < 0.0001$; Time: $F(5, 54) = 144.1$, $p < 0.0001$; Drug \times Time: $F(20, 216) = 13.08$, $p < 0.0001$; b) Drug: $F(4, 216) = 233.2$, $p < 0.0001$; Time: $F(5, 54) = 236.5$, $p < 0.0001$; Drug \times Time: $F(20, 216) = 24.41$, $p < 0.0001$; c) Drug: $F(4, 216) = 244.0$, $p < 0.0001$; Time: $F(5, 54) = 139.8$, $p < 0.0001$; Drug \times Time: $F(20, 216) = 25.93$, $p < 0.0001$; d) Drug: $F(4, 216) = 126.2$, $p < 0.0001$; Time: $F(5, 54) = 77.85$, $p < 0.0001$; Drug \times Time: $F(20, 216) = 15.33$, $p < 0.0001$; e) Drug: $F(4, 216) = 113.8$, $p < 0.0001$; Time: $F(5, 54) = 63.58$, $p < 0.0001$; Drug \times Time: $F(20, 216) = 11.36$, $p < 0.0001$.

scores (Figure 5d). After the last administration of flavopiridol on day 15, the significant attenuation of pain behaviours remained on day 20 (paw withdrawal threshold ($p < 0.01$, two-way ANOVA; Figure 5a), paw withdrawal latency ($p < 0.01$; Figure 5b), number of spontaneous flinches ($p < 0.01$; Figure 5c), and activity-related guarding scores ($p < 0.01$; Figure 5d)).

Discussion

Microglia are regarded as the immune cells in the CNS and the PNS, and are activated quickly in response to outside stimuli, surveying the environments with their ramified processes and monitoring synaptic activity and microenvironments. Studies of inflammation pain and neuropathic pain have focused on the early phase of the pathology; little is known about the dynamics of the microglia response for BCP, a chronic pain.^{16,30} In our experiments, *IBA1* mRNA in the ipsilateral spinal horn increased in a time-dependent fashion, and *IBA1* protein (a microglia marker) increased from day 5 to day 20 (Figures 1a to 1c, Figures 3d to 3i). Also, most Ki67⁺/DAPI⁺ cells (in all phases of the cell cycle, excluding the resting phase, Figures 2a to 2f) and p-HisH3⁺/DAPI⁺ cells (in G₂/M phase of the cell cycle, Figures 2g to 2l) were labelled with *IBA1*, which means that resident

microglia proliferate under the BCP condition. Activated microglia produce and release a series of diffusible factors, including interleukin (IL)-1 β , IL-6, tumour necrosis factor alpha (TNF- α), protease, and nitric oxide in response to outside stimuli via cognate receptors.¹² These factors influence spinal neuronal function via direct or indirect actions. Microglia contract presynaptic terminals and dendritic spines, extending neuronal excitation and contributing to neuronal plasticity.^{31,32}

Minocycline inhibited microglia activity selectively. Behaviourally, rats with BCP treated with minocycline (i.t.) showed a dose-dependent recovery in the decreased paw withdrawal threshold (Figure 1d), paw withdrawal latency (Figure 1e), limb use scores (Figure 1h), or in the increased number of spontaneous flinches (Figure 1f), and activity-related guarding scores (Figure 1g). After the last administration of minocycline on day 15, the significant attenuation of pain behaviours remained on day 20 (Figures 1d to 1h). Therefore, these results suggest that microglia proliferation contributes to pain behaviour in BCP rats. It is possible that inhibition of proliferated microglia may relieve pain behaviour in BCP.

Cyclins and their kinase partners regulate cell cycle progression. Disruption of restriction-point control may

be a common biological feature in clinical treatment. There are two families of cyclins, the cyclin D family (D1, D2, and D3) and the cyclin E family (E1 and E2). Importantly, cyclin D1 regulated the proliferation of spinal astrocytes in a rat model of neuropathic pain.⁹ The failure of tumours in the cyclin D1-deficient animals to progress to higher grades was correlated with a failure to fully activate microglia in the tumour microenvironment.³³ Cyclin D1 is the biomarker protein expressed in G1 or G2/M transition. Compared with the sham controls, the mRNA (Figure 3a) and protein (Figures 3b and 3c) of cyclin D1 increase started at five days after carcinoma cell injection. The number of cyclin D1⁺/DAPI⁺ cells in the ipsilateral dorsal horn increased significantly in a time-dependent manner, starting at day 10 after BCP, and peaking at day 20 ($p < 0.001$, one-way ANOVA; Figures 3d to 3i). Most cyclin D1⁺/DAPI⁺ cells were colocalized with microglia (Figures 3d to 3i). The pool of microglia (IBA1⁺ cells) was already diminished at postnatal day 3 in the absence of cyclin D1, while the number of astrocytes remained unchanged in the cerebral cortex.³⁴ Based on these results, we concluded that cyclin D1 regulates the proliferation of microglia in a rat model of BCP, and the proliferation of astrocytes in a rat model of neuropathic pain.^{9,35} This discrepancy might be explained by different animal models (BCP versus chronic constrictive injury), treatment regimen (female SD rats versus male Wistar rats), and different timepoints (day 20 vs day 10).

Flavopiridol is a cell cycle inhibitor that inhibits glia proliferation in vivo and in vitro.⁹ Flavopiridol reduces cyclin D1 mRNA transcription, and arrests cells in G1 or G2/M transition.²⁹ In our experiment, flavopiridol attenuated the increase of the mRNA (Figure 4a) and protein (Figures 4b and 4c) of cyclin D1, and decreased the number of IBA1⁺/DAPI⁺ cells, cyclin D1⁺/DAPI⁺ cells, and cyclin D1⁺/IBA1⁺/DAPI⁺ cells in the ipsilateral dorsal horn significantly (Figures 4d to 4f). Also, flavopiridol decreased the number of Ki67⁺/DAPI⁺ cells, Ki67⁺/IBA1⁺/DAPI⁺ cells, p-HisH3⁺/DAPI⁺ cells, and p-HisH3⁺/IBA1⁺/DAPI⁺ cells in the ipsilateral dorsal horn (Figures 4g to 4i). We concluded that flavopiridol inhibited the microglia proliferation by reducing cyclin D1 in BCP rats.

Cell cycle modulation may provide an effective therapeutic strategy to reduce hyperpathia after spinal cord injury.³⁶ Cyclin D1 is the marker protein of G1 or G2/M transition. The number of cyclin D1⁺/DAPI⁺ cells in the ipsilateral dorsal horn increased significantly and most cyclin D1⁺/DAPI⁺ cells were colocalized with microglia (Figure 3). If cyclin D1 regulates pain behaviour, disruption of this cell cycle should recover the pain threshold. In our study, flavopiridol, a cell cycle inhibitor, prevented the decrease of paw withdrawal threshold, paw withdrawal latency, limb use scores, or the increase of spontaneous flinches, activity-related guarding scores (Figure 5). After the last administration of flavopiridol on day 15, the significant attenuation of pain

behaviours remained on day 20, excluding limb use scores (Figure 5). Therefore, these results suggest that cyclin D1 contributes to pain behaviour in BCP rats, and disruption of this cell cycle recovers the pain threshold.

In conclusion, our results revealed that the inhibition of spinal microglial proliferation was associated with a decrease in pain behaviour in a rat model of BCP. Cyclin D1 acts as a key regulator of the proliferation of spinal microglia in BCP rats. Disruption of cyclin D1, the restriction-point control of cell cycle, could inhibit the proliferation of microglia and attenuate the pain behaviour in BCP rats. Our findings suggest that cyclin D1 and the proliferation of spinal microglia may be potential targets for the clinical treatment of BCP.

Supplementary material



ARRIVE checklist and additional experiment details.

References

- Goblirsch MJ, Zwolak P, Clohisy DR. Advances in understanding bone cancer pain. *J Cell Biochem.* 2005;96(4):682–688.
- van den Beuken-van Everdingen MHJ, de Rijke JM, Kessels AG, Schouten HC, van Kleef M, Patijn J. Prevalence of pain in patients with cancer: a systematic review of the past 40 years. *Ann Oncol.* 2007;18(9):1437–1449.
- Choi JY, Lee YS, Shim DM, Lee YK, Seo SW. GNAQ knockdown promotes bone metastasis through epithelial-mesenchymal transition in lung cancer cells. *Bone Joint Res.* 2021;10(5):310–320.
- Choi JY, Lee YS, Shim DM, Seo SW. Effect of GNAQ alteration on RANKL-induced osteoclastogenesis in human non-small-cell lung cancer. *Bone Joint Res.* 2020;9(1):29–35.
- Hu X, Fujiwara T, Houdek MT, et al. Impact of racial disparities and insurance status in patients with bone sarcomas in the USA: a population-based cohort study. *Bone Joint Res.* 2022;11(5):278–291.
- Tsoi KM, Gokgoz N, Darville-O'Quinn P, et al. Detection and utility of cell-free and circulating tumour DNA in bone and soft-tissue sarcomas. *Bone Joint Res.* 2021;10(9):602–610.
- Wang C, Xu K, Wang Y, et al. Spinal cannabinoid receptor 2 activation reduces hypersensitivity associated with bone cancer pain and improves the integrity of the blood-spinal cord barrier. *Reg Anesth Pain Med.* 2020;45(10):783–791.
- Paolicelli RC, Bolasco G, Pagani F, et al. Synaptic pruning by microglia is necessary for normal brain development. *Science.* 2011;333(6048):1456–1458.
- Tsuda M, Kohro Y, Yano T, et al. JAK-STAT3 pathway regulates spinal astrocyte proliferation and neuropathic pain maintenance in rats. *Brain.* 2011;134(Pt 4):1127–1139.
- Biber K, Tsuda M, Tozaki-Saitoh H, et al. Neuronal CCL21 up-regulates microglia P2X4 expression and initiates neuropathic pain development. *EMBO J.* 2011;30(9):1864–1873.
- Raghavendra V, Tanga F, DeLeo JA. Inhibition of microglial activation attenuates the development but not existing hypersensitivity in a rat model of neuropathy. *J Pharmacol Exp Ther.* 2003;306(2):624–630.
- Colburn RW, DeLeo JA, Rickman AJ, Yeager MP, Kwon P, Hickey WF. Dissociation of microglial activation and neuropathic pain behaviors following peripheral nerve injury in the rat. *J Neuroimmunol.* 1997;79(2):163–175.
- Bu H, Shu B, Gao F, et al. Spinal IFN- γ -induced protein-10 (CXCL10) mediates metastatic breast cancer-induced bone pain by activation of microglia in rat models. *Breast Cancer Res Treat.* 2014;143(2):255–263.
- Guan X, Fu Q, Xiong B, et al. Activation of PI3K γ /Akt pathway mediates bone cancer pain in rats. *J Neurochem.* 2015;134(3):590–600.
- Guan X-H, Fu Q-C, Shi D, et al. Activation of spinal chemokine receptor CXCR3 mediates bone cancer pain through an Akt-ERK crosstalk pathway in rats. *Exp Neurol.* 2015;263:39–49.
- Apryani E, Ali U, Wang Z-Y, et al. The spinal microglial IL-10/ β -endorphin pathway accounts for cinobufagin-induced mechanical allodynia in bone cancer pain

- following activation of $\alpha 7$ -nicotinic acetylcholine receptors. *J Neuroinflammation*. 2020;17(1):75.
17. **Ke C, Li C, Huang X, et al.** Protocadherin20 promotes excitatory synaptogenesis in dorsal horn and contributes to bone cancer pain. *Neuropharmacology*. 2013;75:181–190.
 18. **Song Z-P, Xiong B-R, Guan X-H, et al.** Minocycline attenuates bone cancer pain in rats by inhibiting NF- κ B in spinal astrocytes. *Acta Pharmacol Sin*. 2016;37(6):753–762.
 19. **Song Z, Xiong B, Zheng H, et al.** STAT1 as a downstream mediator of ERK signaling contributes to bone cancer pain by regulating MHC II expression in spinal microglia. *Brain Behav Immun*. 2017;60:161–173.
 20. **Yaksh TL, Rudy TA.** Chronic catheterization of the spinal subarachnoid space. *Physiol Behav*. 1976;17(6):1031–1036.
 21. **Ke C, Li C, Huang X, et al.** Protocadherin20 promotes excitatory synaptogenesis in dorsal horn and contributes to bone cancer pain. *Neuropharmacology*. 2013;75:181–190.
 22. **Pogatzki EM, Raja SN.** A mouse model of incisional pain. *Anesthesiology*. 2003;99(4):1023–1027.
 23. **Hargreaves K, Dubner R, Brown F, Flores C, Joris J.** A new and sensitive method for measuring thermal nociception in cutaneous hyperalgesia. *Pain*. 1988;32(1):77–88.
 24. **Xu B, Liu S-S, Wei J, et al.** Role of spinal cord Akt-mTOR signaling pathways in postoperative hyperalgesia induced by plantar incision in mice. *Front Neurosci*. 2020;14:766.
 25. **Xu B, Mo C, Lv C, et al.** Post-surgical inhibition of phosphatidylinositol 3-kinase attenuates the plantar incision-induced postoperative pain behavior via spinal Akt activation in male mice. *BMC Neurosci*. 2019;20(1):36.
 26. **Xu B, Guan X-H, Yu J-X, et al.** Activation of spinal phosphatidylinositol 3-kinase/protein kinase B mediates pain behavior induced by plantar incision in mice. *Exp Neurol*. 2014;255:71–82.
 27. **Guan X-H, Fu Q-C, Shi D, et al.** Activation of spinal chemokine receptor CXCR3 mediates bone cancer pain through an Akt-ERK crosstalk pathway in rats. *Exp Neurol*. 2015;263:39–49.
 28. **Guan X-H, Lu X-F, Zhang H-X, et al.** Phosphatidylinositol 3-kinase mediates pain behaviors induced by activation of peripheral ephrinBs/EphBs signaling in mice. *Pharmacol Biochem Behav*. 2010;95(3):315–324.
 29. **Swanton C.** Cell-cycle targeted therapies. *Lancet Oncol*. 2004;5(1):27–36.
 30. **Zhou K-X, He X-T, Hu X-F, et al.** XPro1595 ameliorates bone cancer pain in rats via inhibiting p38-mediated glial cell activation and neuroinflammation in the spinal dorsal horn. *Brain Res Bull*. 2019;149:137–147.
 31. **Wilton DK, Dissing-Olesen L, Stevens B.** Neuron-glia signaling in synapse elimination. *Annu Rev Neurosci*. 2019;42:107–127.
 32. **Tozaki-Saitoh H, Tsuda M.** Microglia-neuron interactions in the models of neuropathic pain. *Biochem Pharmacol*. 2019;169:113614.
 33. **Ciznadija D, Liu Y, Pyonteck SM, Holland EC, Koff A.** Cyclin D1 and cdk4 mediate development of neurologically destructive oligodendroglioma. *Cancer Res*. 2011;71(19):6174–6183.
 34. **Nobs L, Baranek C, Nestel S, et al.** Stage-specific requirement for cyclin D1 in glial progenitor cells of the cerebral cortex. *Glia*. 2014;62(5):829–839.
 35. **Zhao B, Pan Y, Xu H, Song X.** Kindlin-1 regulates astrocyte activation and pain sensitivity in rats with neuropathic pain. *Reg Anesth Pain Med*. 2018;43(5):547–553.
 36. **Wu J, Raver C, Piao C, Keller A, Faden AI.** Cell cycle activation contributes to increased neuronal activity in the posterior thalamic nucleus and associated chronic hyperesthesia after rat spinal cord contusion. *Neurotherapeutics*. 2013;10(3):520–538.
- Author information:**
- X. Guan, PhD, Anesthesiologist
 - X. Gong, BSc, Master's Student
 - Z. Y. Jiao, MSc, Master's Student
 - H. Y. Cao, BSc, Master's Student
 - S. Liu, BSc, Master's Student
 - C. Lin, MSc, Chief Physician
 - X. Huang, BSc, Master's Student
 - H. Lan, BSc, Master's Student
- Department of Anesthesiology, The First Affiliated Hospital of Guangxi Medical University, Nanning, China.
- L. Ma, PhD, Department Director, Department of Anesthesiology, The People's Hospital of Guangxi Zhuang Autonomous Region, Nanning, China.
 - B. Xu, MSc, Chief Physician, Department of Rehabilitation, The People's Hospital of Guangxi Zhuang Autonomous Region, Nanning, Guangxi, China.
- Author contributions:**
- X. H. Guan: Writing – review & editing, Funding acquisition, Conceptualization.
 - X. F. Gong: Project administration, Resources.
 - Z. Y. Jiao: Methodology, Investigation.
 - H. Y. Cao: Methodology, Project administration.
 - S. S. Liu: Investigation, Formal analysis.
 - C. X. Lin: Writing – original draft, Validation.
 - X. F. Huang: Software.
 - H. M. Lan: Data curation.
 - L. Ma: Supervision, Validation.
 - B. Xu: Data curation, Visualization, Conceptualization.
- X. Guan and X. Gong are joint first authors.
- X. Guan and B. Xu are joint senior authors.
- Funding statement:**
- The authors disclose receipt of the following financial or material support for the research, authorship, and/or publication of this article: this work was supported by the Natural Science Foundation of Guangxi Zhuang Autonomous Region (No. 2022GXNSFAA035628) and the National Natural Science Foundation of China (No. 81660200).
- ICMJE COI statement:**
- The funders had no role in study design, data collection and analysis, decision to publish, or preparation of the manuscript. The authors declare no conflict of interest.
- Data sharing:**
- The data generated during the current study are available from the corresponding author on reasonable request.
- Acknowledgements:**
- We are grateful to Jin Wei and the Medical Sciences Research Center of the People's Hospital of Guangxi Zhuang Autonomous Region for their kind assistance.
- Ethical review statement:**
- All experimental protocols were approved by the Animal Care and Use Committee of The First Affiliated Hospital of Guangxi Medical University and were in accordance with the Declaration of the National Institutes of Health Guide for Care. We have included an ARRIVE checklist to show that we have conformed to the ARRIVE guidelines.
- Open access funding**
- The authors confirm that the open access fee for this study was self-funded.
- © 2022 Author(s) et al. This is an open-access article distributed under the terms of the Creative Commons Attribution Non-Commercial No Derivatives (CC BY-NC-ND 4.0) licence, which permits the copying and redistribution of the work only, and provided the original author and source are credited. See <https://creativecommons.org/licenses/by-nc-nd/4.0/>